Uptake and UV-Photooxidation of Gas-Phase PAHs on the Surface of Atmospheric Water Films. 1. Naphthalene

Jing Chen, Franz S. Ehrenhauser, Kalliat T. Valsaraj,* and Mary J. Wornat

Cain Department of Chemical Engineering, Louisiana State University, Baton Rouge, Louisiana 70803-7303

Received: April 26, 2006; In Final Form: May 29, 2006

The adsorption and photochemical reaction of naphthalene vapor at the air−water interface of water films (22 μm and 450 μm) were studied in a horizontal flow reactor. Experiments were conducted in the regime where gas-phase mass transfer resistance did not limit the uptake. The equilibrium uptake was dependent on water film thickness only below 1 μm. Bulk water−air and air-to-interface partition constants were estimated from the experiments. The equilibrium partition constant between the water film and air decreased with increasing temperature. Photochemical reaction products were isolated in the water film after exposure to UV light. Four main oxygenated products were identified (1,3-indandione, 1(3*H*)-isobenzofuranone (phthalide), 2H-1-benzopyran-2-one (coumarin), and 1-naphthol). The initial rates of product formation were 46 to 154% larger for the thin film (22 μm) compared to both a thick film (450 μm) and bulk aqueous phase photooxidation. The atmospheric implications of reactions in water films are discussed.

Introduction

Water films on aerosol particles and in the form of atmospheric droplets have been known to affect the processing of organic compounds in the atmosphere.[1,2] In a recent work, Sumner et al.[3] summarized the interactions of thin films of water with various substrates of atmospheric interest and showed that on most surfaces water films can support a variety of heterogeneous reactions. Reactions that occur at very low rates in the homogeneous gas phase are known to proceed much faster on film surfaces via heterogeneous processes,[4] for which the determining factor is the concentration of compounds in thin films. The uptake depends on the air-to-interface partition constant of the organic compound, its hydrophobicity and the presence of other surface-active compounds in thin films. Reactions of organic vapors on the surface of thin films can also lead to the production of secondary organic aerosols (SOA).[5] A major fate process for chemicals in both bulk and interface regions is the photochemical reaction initiated by solar UV radiation. There have been recent reports on the photochemistry of several compounds in ice and snow.[6−8]

The air/water interface, including both bulk air/bulk water interface and bulk air/water dispersion (rain, fog, mist, snow, ice, and aerosol) interface, is the largest interface in the atmosphere. Figure 1 shows the main physicochemical processes which occur at this interface. As shown in Figure 1, two major processes occur at the air−water interface: mass partitioning and photochemical reactions. Under the specific conditions (air/fog or air/ice) that we are interested in, the ratio of surface area to bulk volume for the water phase can be quite large. As a result, the interfacial effects become significant for the transport and reactions of compounds.

Polycyclic aromatic hydrocarbons (PAHs) are ubiquitous in the atmosphere,[9] and are anthropogenic in origin.[10] Our work focuses on the transport and photochemical transformation characteristics of PAHs at the air/water (fog and ice) interface.

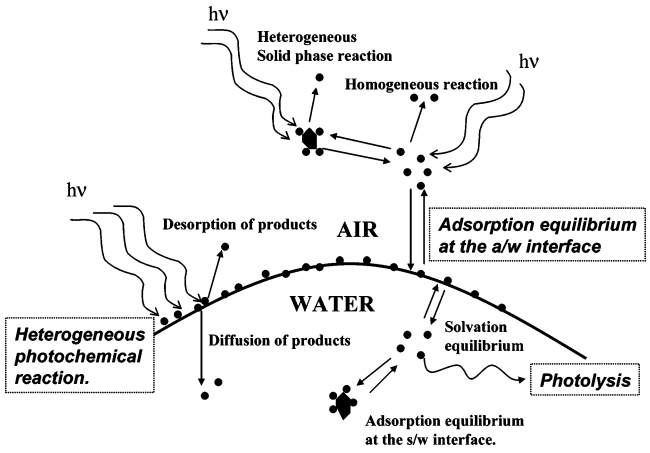

Figure 1. Schematic of the various processes occurring at the environmental air−water interface.

Recent work has shown that large molecular weight hydrocarbons adsorb to the air−water interface and their oxidation rates by gas-phase ozone on micrometer-size water droplets and planar water surfaces are dependent on the surface coverage.[11−16]

Bulk phase photochemical reactions of dissolved PAH compounds with OH radicals generated by UV radiation are well documented and result in ring cleavage.[17,18] Generally, PAHs are stable due to their delocalized π-electron cloud and large resonance energies. Despite their intrinsically low chemical reactivities, PAHs strongly absorb UV light (300−420 nm) and undergo numerous photochemical reactions. The photoreactions of PAHs can be broadly classified into two categories: (i) homogeneous reactions in bulk phases (air, water), and (ii) heterogeneous reactions involving adsorbed PAHs. Homogeneous photoreactions of PAHs have been widely studied, among which the reactions of PAHs with oxygen or ozone in the presence of UV radiation are the most extensively studied.[19−22] Beltran and co-workers investigated the reactions of PAHs dissolved in water under four different conditions (UV radiation, ozonation, oxidation by UV radiation combined with hydrogen

* Corresponding author. E-mail: valsaraj@lsu.edu. Telephone: 2255786522. Fax: 2255781476.

10.1021/jp062560b CCC: $33.50 © 2006 American Chemical Society
Published on Web 07/04/2006

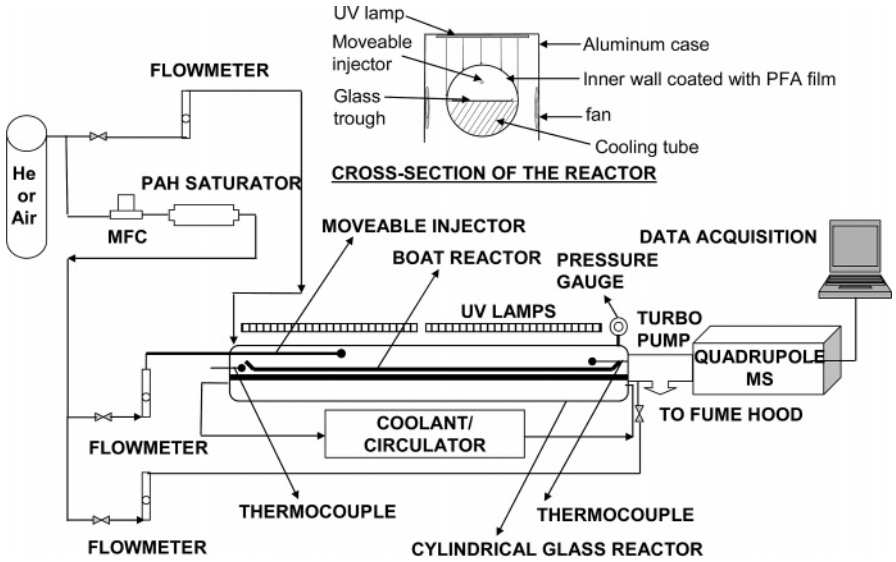

Figure 2. Sketch of the horizontal flow-tube reactor and ancillaries used for carrying out the adsorption and photooxidation experiments.

TABLE 1: Literature Values of the Physicochemical Properties[28] of Naphthalene

property	value	dimension
mol wt	128	g mol^{-1}
aqueous solubility at 298 K	0.097−0.265	mol m^{-3}
vapor pressure (subcooled liquid) at 298 K	0.01−0.03	kPa
bulk water−air Henry's constant, K_{WA} at 298 K[29,30]	33−68	
octanol−water partition constant, K_{ow} at 298 K	$10^{3.29}$−$10^{3.59}$	

peroxide, oxidation by ozone combined with hydrogen peroxide) and reported their kinetics and reaction products.[19−21] Photoreactions of PAHs and alkanes have also been studied under conditions relevant to the prebiotic Earth and the interstellar medium where carbon−carbon bonds have been found to form in the photochemical alkylation of PAHs.[23] Although there are a large number of studies on homogeneous photoreactions of PAHs, there is surprisingly little data on the photooxidation of PAHs under environmentally relevant conditions. Some PAH photoproducts have been obtained using light sources containing high levels of UVC (<280 nm), which is not present in sunlight. McConkey et al.[24] studied the photooxidation of naphthalene in aqueous solution under natural sunlight and determined its photooxidation pathway, but not the kinetics of product formation. Some of the products of UV photolysis are often more toxic than the parent compound.[24,25] The photolysis of PAH compounds adsorbed to ice and water-ice is also reported in the literature.[26] There is some evidence that under stratospheric conditions PAHs react to form higher molecular weight proteinaceous compounds.[23]

The presence of thin water films, or so-called "adlayers", on particulates in the atmosphere opens up the possibility of reactions occurring on the water surface, via adsorption of reactive gases onto the water film; within the water layer, via dissolution of reactive compounds into the condensed phase; and at the solid/water interface. Thus, the presence of water can potentially influence the reactivity at the surface of the aerosol and the extent to which it is able to participate in heterogeneous atmospheric reactions. Recent studies indicate that even small amounts of strongly bound surface-adsorbed water may play a critical role in the interaction of gases with surfaces traditionally presumed to be solids[3]. Compared to gas-phase homogeneous photoreactions, data on heterogeneous photoreactions of PAHs are sparse, especially those at the air−water interface. Mmereki and Donaldson detailed the first study of heterogeneous chemical reactions of PAHs with ozone at the air−aqueous interface.[15,16] There is, however, a lack of data on the photochemical reactivity of PAHs in thin films of water under ambient conditions of temperature and pressure. Hence, this work was undertaken to understand the adsorption and photochemical reactivity of a typical PAH, viz., naphthalene, in thin films of water formed on borosilicate glass surface in a horizontal flow-reactor.

Experimental Section

Naphthalene is the first in the series of PAHs and provides a simple example of potential photoreactions of PAHs in thin water films. Besides, it also has industrial and commercial applications as active ingredients in mothballs, pesticides, crude oils, and gasoline. It is a ubiquitous pollutant in the atmosphere. For example, in the air in Baton Rouge, it has been noted to be the most prevalent PAH molecule.[27] Table 1 lists the physicochemical properties of naphthalene.

The schematic of the apparatus is shown in Figure 2. The reactor is similar to those used in previous work on heterogeneous reactions.[31−33] The flow-tube photoreactor assembly is comprised of a Pyrex tube, a rectangular borosilicate glass channel, a half-circular cooling tube and a removable aluminum block with UV lamps fixed inside of it. The cross-sectional view of the reactor assembly is also shown in Figure 2. The thin water film on which naphthalene was adsorbed and heterogeneous photochemical reactions took place was coated on the bottom surface of the low-edge glass trough (length 0.92 m, width 0.035 m, height 0.005 m, wall thickness 0.0018 m), which was obtained by cutting a rectangular borosilicate glass tubing (Wale Apparatus Co., Hellertown, PA) into halves. The temperature of the water film was maintained by the half-circular copper cooling tube that was placed under the glass trough. A fluid mixture of laboratory grade ethylene glycol (50%) and water (50%) was circulated through the cooling tube by a circulating bath (model 12101-31, Cole-Parmer Co., Vernon

Hills, Illinois) that is capable of controlling temperature in a range of −30 °C to 150 °C. The glass trough and the cooling tube were both contained in the Pyrex tube (length 1 m, o.d. 0.0508m, wall thickness 0.0032m, Chemglass, Vineland, NJ) through which two UV−B lamps (UVP Inc., Upland, CA) delivered UV light of appropriate wavelength (mid range, λ 302 nm). Two fans on the wall of the aluminum block circulated outside air into the block to keep the temperature of the air around the Pyrex reaction tube from getting too high when the UV−B lamps were turned on. Two thermocouples (copper−constantan, SS 304 sheath, 1/16" sheath diameter, Omega Engineering Inc., Stamford, Connecticut) embedded in the cooling tube were in contact with the bottom of the glass trough. They were used to measure the temperature of the water film.

The vapor generator (PAH saturator), shown in Figure 2, was made of two serially connected tubular stainless steel columns (SS 316, 0.013 m o.d., 0.37 m long each), each of which was packed with 15 g of Chromosorb P (60/80 mesh size, acid washed, Supelco Inc., Bellefonte, PA).[34] The Chromosorb P was coated with naphthalene (99.9% purity, Fisher Scientific Co., St. Louis, MO) by mixing it with a naphthalene−hexane solution, and then evaporating hexane. The average loading obtained this way was about 0.02 g of naphthalene per gram of support. The coated packing was loaded into the vapor generation columns with glass wool on both ends of the columns to keep the powder from flowing outside.

Air was used as the carrier gas and a mass flow controller (0−200 mL/min, Aalborg Inc., Orangeburg, NY) was used to obtain reproducible gas flow rates. An in-line stainless steel tube mixer (15 elements, 0.013 m o.d., Cole-Parmer Co., Vernon Hills, IL) was connected with the PAH vapor generator to provide efficient mixing of the PAH vapor and carrier gas. Water vapor was introduced into the reactor to keep the relative humidity 100% in the air and reduce water evaporation during the experiment. A moveable injector (SS 316, o.d. 32 cm) was used to introduce the naphthalene vapor into the glass boat reactor. The temperatures of the liquid and gas were monitored using thermocouples placed close to the surface. The top surface of the half-circular copper cooling tube and the inner top surface of the Pyrex tube were coated with a PFA film (2 mil thick, Berghof America, Coral Springs, FL) to avoid the adsorption of naphthalene onto these surfaces.

A Hewlett-Packard 5890 Series II gas chromatograph with a Hewlett-Packard Mass Selective detector (MSD) was used to analyze the gas stream on-line. A 6-port injection valve (Valco Instrument Co., Houston, TX) and a digital valve sequence programmer (Valco Instrument Co., Houston, TX) were connected to the GC-MS such that the gas-phase sample was injected into the GC-MS automatically. An untreated fused silica tubing (Supelco Inc., Bellefonte, PA) was used as the GC column and the retention time of naphthalene inside the column was reduced to about 0.8 min. With this blank column installed, the gas phase was sampled every 3 min. The injection volume of the gas phase samples was 100 μL, determined by the volume of the sample loop.

A blank experiment was first conducted using the boat without any water film. Either helium or pure air was used to generate the saturated naphthalene stream. The carrier gas containing naphthalene vapor was passed through the movable injector, and the QMS signal was monitored. Thin water films were prepared by coating the bottom surface of the glass trough with a known amount of deionized water (pH = 6.3). To easily obtain a uniform water film, the bottom surface of the glass trough was covered with 50 wt % NaOH solution for 1 h and then washed clean with deionized water. The boat was placed in the cylindrical reactor and allowed to come to equilibrium temperature determined by the coolant inside the cooling tube placed underneath. The gas flow was started and the background QMS signal was recorded. Thereupon, the naphthalene stream in air was introduced through the movable injector, which was placed at the entrance of the reactor. Therefore, the entire reactor was used for adsorption. The reduction in MS signal because of adsorption uptake on the water film was monitored. When adsorption was complete, i.e., when inlet and exit signals matched, the UV lamps were switched on and the photoreaction of naphthalene on the thin film was allowed to occur for a given duration of time. The UV light intensity falling on the reactor was 1.85 W·m^{-2}at the UV−B wavelength of 302 nm. The gas stream was monitored for the change in the naphthalene QMS signal. The liquid in the reactor was collected and analyzed for the product compounds using HPLC. The experiments were repeated for different temperature and water film thickness.

To compare the reactions in water films with that in bulk water, we also conducted experiments in the same reactor but with several small (i.d. 0.0254 m) vials containing 6 mL solution of naphthalene. To keep the conditions similar to the thin film case (constant naphthalene concentration in the liquid phase) we placed pure crystals of naphthalene in the vials during the reaction as was done by McConkey et al.[24]

Quantification of naphthalene and products in the aqueous samples was done using liquid chromatography. Identification of compounds was achieved by matching retention times of standard solutions within ±0.1 min and by matching the UV spectrum of the standards and the sample. The instrument consisted of an Agilent Technologies HPLC 1100 series with online degasser (G1379A), quaternary pump (G1311A), autosampler (G1313A), column thermostat (G1316A), diode array UV detector (G1315B), and mass spectrometer (G1956B) with atmospheric pressure photo ionization (APPI) interface. An Ultra Aqueous C18 column of 0.25 m × 0.0021 m with 5 μm particle size (Restek Corp, USA) was used. The injection volume was 100 μL, and the column thermostat was set to 30 °C. The mobile phase started at 100% ammonia formate buffer pH 3.0; 5 M ammonia formate solution and held for 10 min, then ramped up to 100% methanol within 60 min and held for 15 min at a constant flow rate of 2 × 10^{-7} m^3/min. The detection wavelength was set to 254 nm with 4 nm bandwidth and 4 nm slit.

Results and Discussion

Data Analysis. The QMS signal intensity is related to the apparent dimensionless partition constant (Henry's constant), K_{WA}* for naphthalene between air (gas) and water (film) as follows[31]

$$K_{wa}^* = \frac{I(t)}{S_0} \cdot \frac{Q_g}{V} \tag{1}$$

where $I(t)$ is the area (integral) difference between the baseline signal (S_0) from the blank experiment and the signal from the water film experiment. V is the volume of the water film (m^3) and Q_g is the total volumetric flow rate (m^3·min^{-1}) of the helium stream. Note that K_{WA}* is a composite of the bulk water-air partition constant, K_{WA} (the conventional Henry's constant for absorption) and the air−interface adsorption constant, K_{IA}. Thus,

$$K_{wa}^* = K_{wa} + \frac{K_{IA}}{\delta} \tag{2}$$

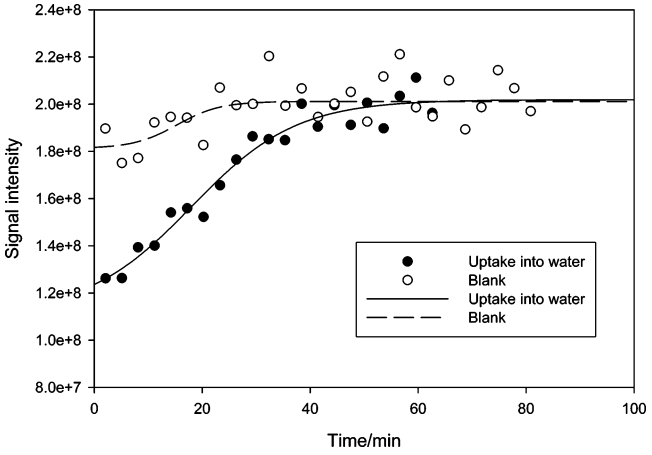

Figure 3. Naphthalene signal for the two cases involving control and water film experiments.

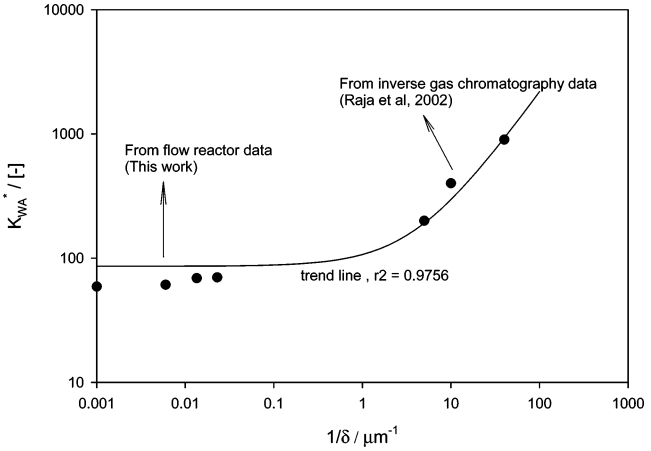

Figure 4. Effect of water film thickness on the partition constant for naphthalene.

where δ is the film thickness. As $\delta \rightarrow \infty$ and/or for small values of K_{IA}, the interfacial adsorption term is not significant and $K_{WA}^* \rightarrow K_{WA}$. For small values of δ, the interfacial adsorption term cannot be neglected.

Figure 3 is a typical naphthalene QMS signal at the exit of the reactor for two cases. The first one is the control experiment where the glass boat reactor was empty, i.e., without any water film and the second one is that in which a 496 μm water film was placed in the glass boat. The injected gas is initially exposed to a fresh surface upon which there is rapid uptake immediately following the downstream of the injection point. This leads to the initial drop in the naphthalene signal at the outlet of the reactor. The maximum value of the concentration corresponds to the inlet gas concentration upstream of the reactor and is reached after uptake equilibrium is reached. The slow rise of the signal to that of the inlet stream shows that the film has reached saturation uptake.

For semivolatile compounds such as naphthalene, the mass transport from the gas phase to an aqueous phase can be gas-phase diffusion limited.[35] The gas-side mass transfer resistance will be lowered as the gas-flow rate (velocity) increases. Increasing gas flow rate therefore should increase the overall mass transfer coefficient. To ascertain the mass transfer regime in the reactor a set of initial experiments was undertaken for a relatively thick film (950 μm). The measured concentration ratio increased with increasing gas flow rate at a temperature of 293 K. We observed that at flow rates larger than 100 mL·min^{-1} there was no discernible change in the partition constant. For the subsequent experiments, the gas flow rate in the reactor was fixed at 100 mL·min^{-1}.

Effect of Water Film Thickness on Partitioning to the Film. The effect of water film thickness on the overall partition constant, K_{WA}^* was studied by varying the water film thickness in the reactor from 45 to 950 μm at a constant temperature of 293K and a flow rate of 100 mL·min^{-1}. The bottom surface of the glass trough was always fully coated with the water film and its surface area was determined ($A_W = 317$ cm^2). Varied water film thicknesses were obtained by changing the volume of the water while keeping the surface area of the film constant. The partition constant increased only slightly with increasing surface area per unit volume, $1/\delta$. The variation in surface area per unit volume was from 10 to 230 cm^{-1} and the corresponding increase in the partition constant was 18.6. In previous work from our laboratory[36] we used an inverse gas chromatography (IGC) technique to obtain very thin water films (0.025 to 0.2 μm) and corresponding K_{WA}^* values varying from 200 to 900 for naphthalene. These two sets of data are plotted in Figure 4. A trend line (linear fit from Microsoft Excel) can be drawn such that as $\delta \rightarrow \infty$ (i.e., $1/\delta \rightarrow 0$), the intercept $K_{WA}^* \rightarrow K_{WA} = 86 \pm 23$. The slope of the line when $1/\delta$ is large gives the air−water interface partition constant, $K_{IA} = 21 \pm 1$ μm. The correlation coefficient for the linear trend line fit ($r^2 = 0.97$) is acceptable. The experimental values at 293 K are compared to available literature values in Table 2. The effect of the interface thickness on the overall partition ratio for naphthalene becomes evident only at $\delta < 1$ μm. Obtaining the precise thickness of the water film for small δ is precluded by the difficulty in creating a uniform thin water film.

Effect of Temperature on Uptake into the Film. The temperature dependence is described by the van't Hoff equation

$$\ln K_{wa}^* = -\frac{\Delta_{g\rightarrow w}H}{R}\cdot\frac{1}{T} + \frac{\Delta_{g\rightarrow w}S}{R} \qquad (3)$$

Experiments were conducted on a 150 μm water film within a temperature range of 278−303K. At this film thickness, *ab*sorption into the bulk phase of the thin film is dominant over the surface *ad*sorption term. At the lowest temperature uptake occurs on a water film only 5K above the freezing temperature. Figure 5 is a plot of $\ln K_{WA}^*$ vs $1/T$ which gives an enthalpy of solvation, $\Delta_{g\rightarrow w}H$ of -22 ± 6 kJ mol^{-1} and an entropy of solvation $\Delta_{g\rightarrow w}S$ of -41 ± 20 J·mol^{-1}·K^{-1}. The correlation coefficient was 0.882, indicating that over the temperature range the fit is satisfactory.

Photochemical Reactions in the Thin Film. Figure 6 shows a typical HPLC chromatogram of a sample of thin water film (450 μm) with adsorbed naphthalene exposed to UV irradiation for 16 h. There are several peaks in the chromatogram, eight of which have been unequivocally identified by matching the UV spectra and retention times with those of authentic reference standards. Our analyses demonstrated that the major photo-oxidation products of naphthalene on thin films were several oxygenated products. We focused on four major products that were always observed in the aqueous samples, these are peaks 1, 2, 3, and 7 identified respectively as 1,3-indandione, 1(3*H*)-isobenzofuranone (phthalide), 2*H*-1-benzopyran-2-one (coumarin), and 1-naphthol. Quantification of compounds was also done on the HPLC.

The mechanisms of photooxidation of PAHs are well established in the literature.[24,37] The possible route for the formation of these compounds is by the addition of oxygen to the naphthalene ring by either [2 + 2] or [2 + 4] photocycloaddition mechanism[24] and shown schematically in Figure 7. The

TABLE 2: Experimental and Literature Values of Partition Constants for Naphthalene at 293 K

parameter	data	reference
air−water bulk phase partition constant, K_{WA}/[-]	86 ± 23	this work
	64	extrapolated from NIST handbook[29]
	72	Alaee et al.[30]
air−water interface partition constant, K_{IA}/μm	21±1	this work
	27±2	Raja et al.[36]

two types of endoperoxides so formed undergo further transformations. Although most oxidizing reactions produced dimerized or larger ring products, none was observed in this work. 1-Naphthol is a major compound obtained from one of the endoperoxides, which has been shown[38] to easily lead to 1,2-naphthoquinone. The endoperoxide can also lead directly to 1,2-naphthoquinone by elimination of a molecule of H_2. Naphthoquinone was observed in some of our samples. However, it was quickly subjected to further chemical reactions, and did not accumulate in sufficient concentration to be detected in our analytical system under all conditions. 1,2-Naphthoquinone is known to lead to the formation of coumarin. Although coumarin is known[39] to form dimers under certain conditions, no such dimers were detected in our system. The [2 + 4] cycloaddition endoperoxide is known to form 1(3*H*)-isobenzofuranone (phthalide) upon photolysis by elimination of an acetylene molecule, which is known to be a stable compound. The [2 + 4] cycloaddition product also is known[40] to produce 1,4-naphthaquinone

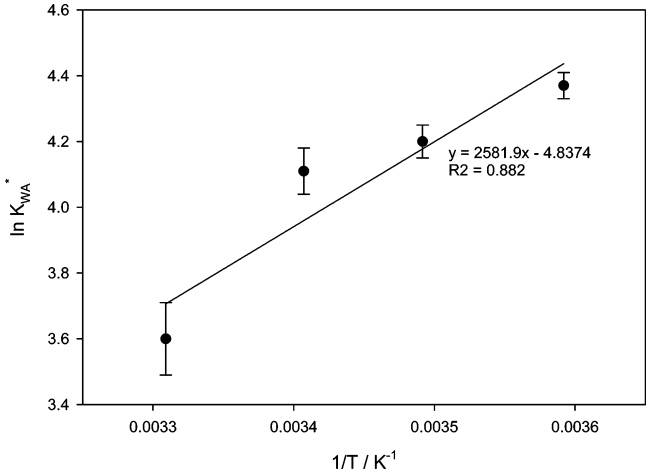

Figure 5. Effect of temperature on the naphthalene partitioning to the thin film.

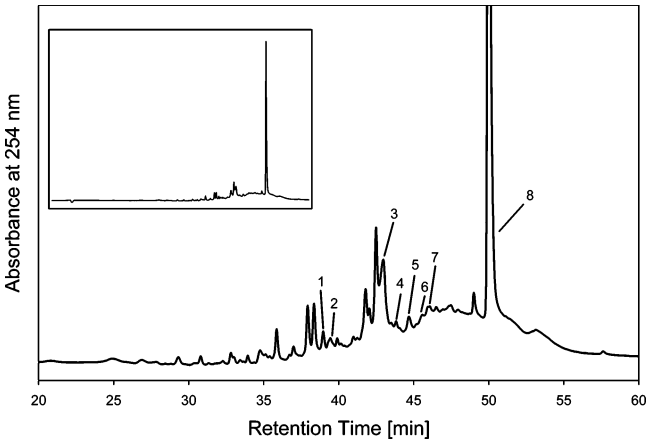

Figure 6. Detailed HPLC trace of the aqueous film sample after 16 h exposure to UV light (full HPLC trace is the inset). The compounds identified are 1,3-indandione (**1**), phthalide (**2**), coumarin (**3**), 1-indanone (**4**), 1,4-naphthoquinone (**5**), 2-naphthol (**6**), 1-naphthol (**7**), and naphthalene (**8**).

which easily undergoes hydroxylation and a carbon atom loss leading to 1,3-indandione. Thus, in the UV photodegradation of naphthalene some products are unstable intermediates while others are stable products.

As stated in our previous work,[36] there is a substantial free energy minimum (−24 kJ/mol) for naphthalene adsorption at the air/water interface from the gas phase. This is equivalent to a 16 000 times enrichment at the interface over the gas phase. It has been reported by Vacha et al.[41] that molecular dynamics simulations showed that oxygen also has a free energy minimum of −0.5 kJ/mol for adsorption at 300 K which translates to a 240% enhancement of O_2 at the interface compared to the gas phase. Thus, it can be hypothesized that the reaction starts by adsorption of naphthalene and reaction with oxygen at the air−water interface to form either a [2+2] or a [2+4] adduct molecule as shown in Figure 7. The adduct molecule further reacts and converts to products that are water-soluble and have very low volatility (Figure 7). The reactor data can be explained based on the following "global" mechanism:

$$\mathrm{N} \underset{k_1}{\overset{h\nu}{\Longrightarrow}} \mathrm{P1} \underset{k_2}{\overset{h\nu}{\Longrightarrow}} \mathrm{P2}$$

where N is the adsorbed naphthalene, and P1 and P2 are products of photoreaction. Note that both k_1 and k_2 in the above scheme are overall rate constants that include the photochemistry in the bulk phase and surface reactions.[42] For the special case where the amount of N is constant the overall rate of product formation is given by[43]

$$C_{\mathrm{P1}}(t) = \frac{k_1}{k_2} C_{\mathrm{N0}}[1 - \mathrm{e}^{-k_2 t}] \tag{4}$$

Thus, for this general case, the product concentration exponentially reaches a constant value given by $(k_1/k_2)C_{N0}$. If P1 is a stable product, further degradation can be neglected. In this case, one obtains

$$C_{\mathrm{P1}}(t) = k_1 C_{\mathrm{N0}} t \tag{5}$$

Thus for the special case where P1 is a stable product, a linear increase in product concentration with time will be noted. Fitting the data to eq 5 will give k_1 and k_2 for a specific product.

Figures 8 and 9 show the change in the concentration of various products and naphthalene in the liquid phase as a function of time for reactions respectively in a thick film (450 μm) and a thin film (22 μm). In each case, the average of five replicate experiments is shown. The concentration of three products (coumarin, 1,3-indandione and 1-naphthol) reached a maximum whereas that of phthalide continued to increase. The rate constants of formation of products (k_1) and their dissipation (k_2) obtained by fitting data to eq 5 are given in Table 3. The fit to the nonlinear equation was good in all cases. The rate constant for the formation of the product from naphthalene, k_1, was in all cases larger for the thin film than for the thick film case. In other words, k_1 was larger when the surface area per unit volume of the water film ($1/\delta$) increased, indicating contribution from heterogeneous reactions. Moreover, for the

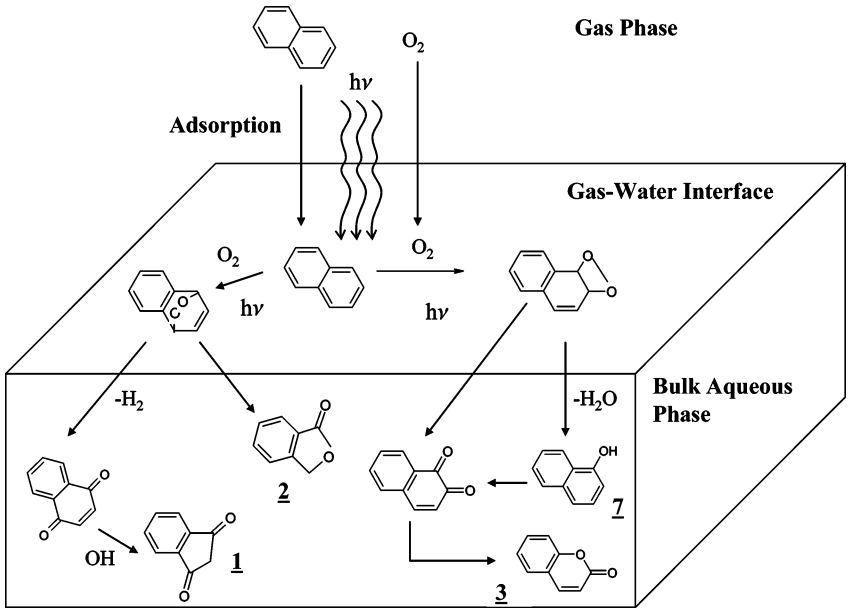

Figure 7. Mechanisms for the formation of main products identified in the HPLC trace of the aqueous film samples.

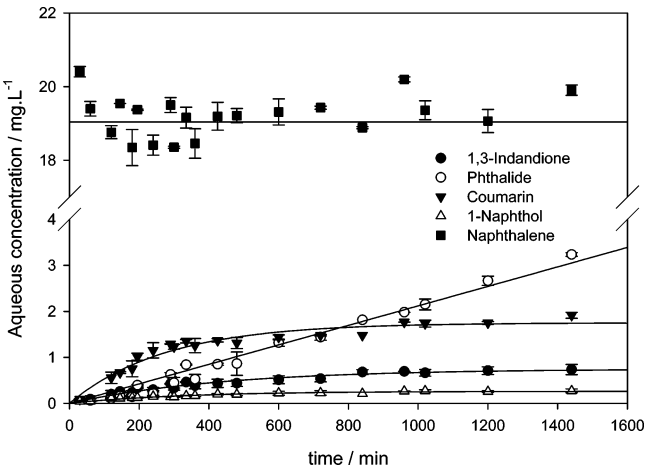

Figure 8. Photooxidation of naphthalene vapor on a 450 μm water film.

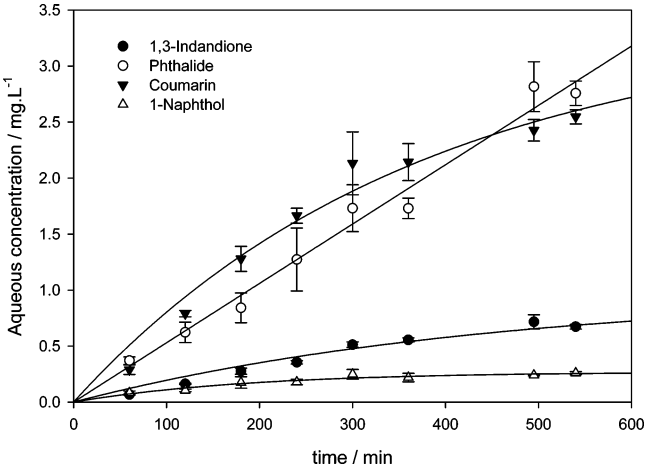

Figure 9. Photooxidation of naphthalene vapor on a 22 μm water film.

bulk reaction, we observed that the rate constants were very similar to those for the thick film reaction. Increases of 30% (coumarin), 192% (phthalide), 31% (indandione), and 80% (1-naphthol) were observed as the surface area per unit volume increased 568-fold.

The measured *initial* rate of product formation in the flow reactor is given by

$$+r_{P0} = k_{homo}C_{N0} + k_{hetero}\frac{\Gamma_{N0}}{\delta} \qquad (6)$$

where Γ_{N0} (mol·m^{-2}) is the surface concentration of naphthalene, δ is the film thickness (m), and C_{N0} is the bulk aqueous phase concentration of naphthalene (mol·m^{-3})·k_{homo} (min^{-1}) is the homogeneous (bulk liquid phase) reaction rate constant and k_{hetero} (min^{-1}) is the heterogeneous (surface) reaction rate constant. Since, $\Gamma_{N0} = (K_{IA}/K_{WA})C_{N0}$, we can rewrite the above equation as

$$+r_{P0} = \left(k_{homo} + \frac{k_{hetero}}{\delta}\cdot\frac{K_{IA}}{K_{WA}}\right)C_{N0} \qquad (7)$$

We established earlier that surface effects are negligible for bulk (or thick film) reactions, which therefore, give us directly the value of $k_{homo} = k_{1,bulk}$. Using eq 7 the value of k_{hetero} can be calculated from the overall k_1 obtained for the thin film reaction. The values of k_{hetero} (min^{-1}) obtained were 9.9×10^{-3} (coumarin), 1.66×10^{-3} (phthalide), 2.3×10^{-3} (indandione), and 3.0×10^{-3} (1-naphthol).

Atmospheric Implications. In films of water that comprise aerosols and fog, reactions can be expected to occur similar to those observed in thin water films. The rates of product formation in water films can rival or exceed those observed in bulk water reactions. In the atmosphere, the loss of naphthalene via photooxidation in thin water films on particles and dispersoids should be weighed against other dominant reaction loss processes. The competing reactions include (i) the homogeneous gas-phase oxidation of naphthalene by photochemically generated hydroxyl radical and (ii) the heterogeneous oxidation of adsorbed naphthalene on solid particles by photochemically generated gas-phase hydroxyl radical. Let us consider 1 m^3 of air containing 1 ppm$_v$ of gas-phase naphthalene and estimate the reaction lifetime in the atmosphere due to the three processes considered above.

TABLE 3: Kinetic Rate Constants for Product Formation in Water Films in the Reactor[a]

	thin film (22 μm) reaction ($1/\delta = 4.54 \times 10^4\ m^{-1}$)			thick film (450 μm) reaction ($1/\delta = 2.2 \times 10^3\ m^{-1}$)			bulk liquid reaction ($1/\delta = 80\ m^{-1}$)		
compound	k_1/min^{-1}	k_2/min^{-1}	R^2	k_1/min^{-1}	k_2/min^{-1}	R^2	k_1/min^{-1}	k_2/min^{-1}	R^2
coumarin	4.8×10^{-4}	2.7×10^{-3}	0.969	3.3×10^{-4}	3.6×10^{-3}	0.945	3.7×10^{-4}	4.0×10^{-3}	0.982
phthalide	2.8×10^{-4}		0.981	1.1×10^{-4}		0.976	9.6×10^{-5}		0.991
1,3-indandione	1.1×10^{-4}	2.2×10^{-3}	0.956	8.7×10^{-5}	2.2×10^{-3}	0.950	8.4×10^{-5}	2.3×10^{-3}	0.972
1-naphthol	7.4×10^{-5}	5.2×10^{-3}	0.927	4.3×10^{-5}	3.1×10^{-3}	0.952	4.1×10^{-5}	3.4×10^{-3}	0.903

[a] R^2 is the correlation coefficient for the data fit to eq 5.

The lifetime due to homogeneous oxidation in air by hydroxyl radical is given by

$$\tau_1 = \frac{1}{k_{OH}[OH^\bullet]} \tag{8}$$

where k_{OH} is the second-order reaction rate constant of naphthalene with OH• ($= 2.2 \times 10^{-17}\ m^3 \cdot molecule^{-1} \cdot s^{-1}$). Adopting a typical atmospheric [OH•] of 1.4×10^{12} molecules·m^{-3}, we derive $\tau_1 = 9$ h.

The lifetime due to heterogeneous oxidation of naphthalene adsorbed on solid particles by photochemically generated OH radicals in air is given by[44]

$$\tau_2 = \frac{C_g}{-r_{het,s}} = \frac{C_g}{\omega \frac{\gamma}{4} A_N [OH^\bullet]} \tag{9}$$

where ω is the thermal velocity of the hydroxyl radical (=661 m·s^{-1}). γ is the reaction probability of OH• with adsorbed naphthalene molecule which is taken to be 0.5 consistent with experimental data for PAHs.[45] Assuming a molecular cross section of 0.5 nm^2 for a naphthalene molecule, the surface area concentration of naphthalene, A_N was estimated to be 12 m^2·m^{-3}. This gives a value of $\tau_2 = 4.8$ h.

The lifetime due to UV photochemical reaction of naphthalene adsorbed on a water film is given by the following equation

$$\tau_3 = \frac{C_g}{r_p^0} = \frac{1}{\left(k_{homo} + \frac{k_{hetero}}{\delta} \cdot \frac{K_{IA}}{K_{WA}}\right) \cdot K_{WA}} \tag{10}$$

Consider, for example, the experimental values of the *initial* rate constants for the formation of coumarin from naphthalene described in Table 3. Using the values of K_{IA} (=21 μm) and K_{WA} (=86) obtained earlier, and values of k_{homo} ($=3.7 \times 10^{-4}$ min^{-1}) and k_{hetero} ($=9.9 \times 10^{-3}$ min^{-1}) for a δ of 15 μm gives $\tau_3 = 22$ min.

It is evident from the above calculation that UV-initiated photochemical reactions in water films can compete with other reaction losses and may be of significance on atmospheric particles and dispersions (fog, mist). However, one should caution that these estimates are only preliminary. It is well-known that dissolved organic compounds (DOCs) such as humic and fulvic acids in natural water can affect the photochemical reactions.[46] Therefore, to what extent the reaction lifetime of a PAH such as naphthalene will be affected because of DOC should be investigated before extrapolating our results to the natural environment.

Acknowledgment. This work was supported by a grant from the National Science Foundation (ATM 0355291). The Air Force Office of Scientific Research is gratefully acknowledged for the HPLC/UV/MS instrument, purchased through Grant FA9550-05-1-0253.

References and Notes

(1) Hunt, S. W.; Roeselova, M.; Wang, W.; Wingen, L. M.; Knipping, E. M.; Tobias, D. J.; Dabdub, D.; Finlayson-Pitts, B. J. *J. Phys. Chem. A* **2004**, *108*, 11559−11572.
(2) Ewing, G. W. *Chem. Rev.* **2006**, *106*, 1511−1526.
(3) Sumner, A. L.; Menke, E. J.; Dubowski, Y.; Newberg, J. T.; Penner, R. M.; Hemminger, J. C.; Wingen, L. M.; Brauers, T.; Finlayson-Pitts, B. J. *Phys. Chem. Chem. Phys.* **2004**, *6*, 604−613.
(4) Strekowski, R. S.; Remorov, R.; George, Ch. *J. Phys. Chem. A* **2003**, *107*, 2497−2504.
(5) Blando, J. D.; Turpin, B. J. *Atmos. Environ.* **2000**, *34*, 1623−1632.
(6) Domine, F.; Shepson, P. B. *Science* **2002**, *297*, 1506−1510.
(7) Dubowski, Y.; Hoffman, M. R. *Geophys. Res. Lett.* **2000**, *27*, 3321−3324.
(8) Klanova, J.; Klan, P.; Nosek, J.; Holoubek, I. *Environ. Sci. Technol.* **2003**, *37*, 1568−1574.
(9) Bernstein, M. P.; Dworkin, J. P.; Sandford, S. A.; Allamandola, L. J. *Adv. Space Res.* **2002**, *30*, 1501−1508.
(10) Hafner, W. D.; Carlson, D. L.; Hites, R. A. *Environ. Sci. Technol.* **2005**, *39*, 7374−7379.
(11) Raja, S.; Valsaraj, K. T. *J. Air Waste Manage. Assoc.* **2005**, *55*, 1345−1355.
(12) Raja, S.; Valsaraj, K. T. *Environ. Sci. Technol.* **2004**, *38*, 763−768.
(13) Raja, S.; Valsaraj, K. T. *J. Air Waste Manage. Assoc.* **2004**, *54*, 1550−1559.
(14) Donaldson, D. J.; Mmereki, B. T.; Chaudhuri, S. R.; Handley, S.; Oh, M. *Faraday Discuss.* **2005**, *130*, 1−13.
(15) Mmereki, B. T.; Donaldson, D. J. *J. Phys. Chem. A* **2003**, *107*, 11038−11042.
(16) Mmereki, B. T.; Donaldson, D. J.; Gilman, J. B.; Eliason, T. L.; Vaida, V. *Atmos. Environ.* **2004**, *38*, 6091−6103.
(17) Debestani, R.; Ivanov, I. N. *Photochem. Photobiol.* **1999**, *70*, 10−34.
(18) Finalayson-Pitts, B. J.; Pitts, J. N., Jr. *Science* **1997**, *276*, 1045−1051.
(19) Beltran, F. J.; Ovejero, G.; Garcia-Araya, J. F.; Rivas, J. *Ind. Eng. Chem. Res.* **1995**, *34*, 1607−1615.
(20) Beltran, F. J.; Ovejero, G.; Rivas, J. *Ind. Eng. Chem. Res.* **1996**, *35*, 883−890.
(21) Beltran, F. J.; Gonzalez, M.; Rivas, J. *J. Environ. Sci. Health* **1996**, *A31*, 2193−2210.
(22) Miller, J. S.; Olejnik, D. *Wat. Res.* **2001**, *35*, 233−243.
(23) Mahajan, T. B.; Elsila, J. E.; Deamer, D. W.; Zare, R. N. *Origins Life Evol. Biosphere* **2003**, *33*, 17−35.
(24) McConkey, B. J.; Hewitt, L. M.; Dixon, D. G.; Greenberg, B. M. *Water, Air Soil Pollut.* **2002**, *136*, 347−359.
(25) Arey, J.; Atkinson, R.; Harger, W. P.; Helmig, D.; Sasaki, J. *Formation of mutagens from the atmospheric photooxidation of PAH and their occurrence in ambient air*; Statewide Air Pollution Research Center, University of California: Riverside, CA, 1994.
(26) Bernstein, M. P.; Sandford, S. A.; Allamandola, L. J.; Gilletter, J. S.; Clemett, S. J.; Zare, R. N. *Science* **1999**, *283*, 1135−1138.
(27) Subramanyam, V.; Valsaraj, K. T.; Thibodeaux, L. J.; Reible, D. *Atmos. Environ.* **1994**, *28*, 3083−3091.
(28) Montgomery, J. H. *Groundwater Chemicals: Desk Reference*; 2nd ed.; CRC Press/Lewis Publishers: Boca Raton, FL, 1996.
(29) Sander, R. Henry's Law data. *NIST Chemistry WebBook, NIST Standard Reference Database*, 69th ed.; Lindstrom, P. J., Mallard, W. G., Eds.; U.S. Department of Commerce: Gaithersburg, MD, 2005.
(30) Alaee, M.; Whittal, R. M.; Strachan, W. M. J. *Chemosphere* **1996**, *32*, 1153−1164.

(31) Strekowski, R. S.; George, C. *J. Chem. Eng. Data* **2005**, *50*, 804−810.
(32) Finlayson-Pitts, B. J.; Pitts, J. N., Jr. *Chemistry of the Upper and Lower Atmosphere: Theory, Experiments and Applications*; 2nd ed.; John Wiley & Sons: New York, 2000.
(33) Behr, P.; Terziyski, A.; Zellner, R. *Z. Phys. Chem.* **2004**, *218*, 1307−1327.
(34) Raja, S. Ph.D. Dissertation. LSU, Baton Rouge, LA, 2005.
(35) Smith, J. H.; Bomberger, D. C.; Haynes, D. L. *Chemosphere* **1981**, *10*, 281−289.
(36) Raja, S.; Yaccone, F. S.; Ravikrishna, R.; Valsaraj, K. T. *J. Chem. Eng. Data* **2002**, *47*, 1213−1219.
(37) Fasnacht, M. P.; Blough, N. V. *Environ. Sci. Technol.* **2003**, *37*, 5767−5772.
(38) Karthikeyan, K. G.; Chorover, J. *Environ. Sci. Technol.* **2000**, *34*, 2939−2946.
(39) Hammond, G. S.; Stout, C. A.; Lamola, A. A. *J. Am. Chem. Soc.* **1964**, *86*, 3103−3106.
(40) Pramauro, E.; Prevot, A. B.; Vincenti, M.; Brizzolesi, G. *Environ. Sci. Technol.* **1997**, *31*, 3126−3131.
(41) Vacha, R.; Slavicek, P.; Mucha, M.; Finlayson-Pitts, B. J.; Jungwirth, P. *J. Phys. Chem. A* **2005**, *108*, 11573−11579.
(42) Poschl, U.; Letzel, T.; Kramer, L.; Niessner, R. *J. Aerosol Sci.* **1999**, *30*, S871−S872.
(43) Levenspiel, O. Chemical Reaction Engineering. *Ind. Eng. Chem. Res.* **1999**, *38*, 4140−4143.
(44) Wayne, R. P. *Chemistry of Atmospheres*; 3rd ed.; Oxford University Press: New York, 2000.
(45) Bertram, A.; Ivanov, A. V.; Hunter, M.; Molina, L. T.; Molina, M. J. *J. Phys. Chem. A* **2001**, *105*, 9415−9421.
(46) Donaldson, D. J.; Vaida, V. *Chem. Rev.* **2006**, *106*, 1445−1461.